

Detection of Brain Tumors Based on Automatic Symmetry Analysis

Pavel Dvorak

Department of Telecommunications
Faculty of Electrical Engineering and Communication
Brno University of Technology, 612 00 Brno, Czech Republic
pavel.dvorak@phd.feec.vutbr.cz

Walter Kropatsch

Pattern Recognition and Image Processing Group
Institute of Computer Graphics and Algorithms
Faculty of Informatics
Vienna University of Technology, Favoritenstr. 9/186-3, A-1040 Vienna, Austria
krw@prip.tuwien.ac.at

Abstract. *This article focuses on the detection of a brain tumor location in magnetic resonance images. The aim of this work is not the precise segmentation of the tumor and its parts but only the detection of its approximate location. It will be used in future work for more accurate segmentation. For this reason, it also does not deal with detecting of the images containing the tumor. The algorithm expects a 2D T2-weighted magnetic resonance image of brain containing a tumor. The detection is based on locating the area that breaks the left-right symmetry of the brain. The created algorithm was tested on 73 images containing tumor, tumor with edema or only edema. These pathological structures had various sizes and shapes and were located in various parts of the brain.*

1. Introduction

The detection of brain tumors is generally a more complex task than the detection of any other image object. Pattern recognition usually relies on the shape of the required objects. But the tumor shape varies in each case so other properties have to be used. The general properties of healthy brain are widely used as a prior-knowledge. One of them is the probability of tissues locations using probability brain atlas, which is used e.g. in [7]. Another widely used knowledge, which is used in this article, is the approximate left-right symmetry of healthy

brain. This approach is also used e.g. in [3] [4] [5]. Areas that break this symmetry are most likely parts of a tumor.

There are also many other methods used for tumor extraction, but they usually rely on machine learning algorithms such as SVM used e.g. in [6]. For this purpose, many algorithms need to have patient-specific training dataset. This makes the method more demanding for the experts. These methods usually rely on other contrast images, such as T1-weighted contrast enhanced images [10]. Fully automatic exact segmentation of the tumor is still an unsolved problem, as the accurate image segmentation itself. The method proposed in this work is less accurate than many other methods used nowadays, but it is fully automatic and it is used only for the detection of the brain tumor location for subsequent segmentation, which will be the aim of future work.

The big advantage of the symmetry approach is that the process does not need any intensity normalization, human work etc. The only step that needs to be done is the symmetry axis detection. Another advantage is its independence on the type of the tumor. It can correctly detect anomalies in images containing a tumor, a tumor with edema or only an edema, which is an abnormal accumulation of the fluid around the tumor and is present only with particular types of tumors.

2. Proposed Method

The input of the whole process is a stand-alone 2D T2-weighted magnetic resonance image containing a tumor. It means that no neighbor slices are considered. The reason for T2-weighted image is the visibility of tumors in this type of image.

The tumor detection process consists of several steps. The first step is the brain extraction followed by cutting the image. In this cut image, the asymmetric parts are detected and then the decision which half contains the tumor is made. The detection of the symmetry axis is skipped because the input data were aligned in previous processing. The only assumption of proposed method is a vertically aligned head. For the purpose of detecting the symmetry axis, the well performed algorithm works and is described in [8]. Addition of this method as a preprocessing step will be one of the aims of the future work.

2.1. Brain Extraction

The extraction of skull is based on technique mentioned in [2] and is done by the well-known method called Active contour, or Snakes [9]. At first, the smallest rectangle, whose sides are parallel to the image sides, surrounding the skull are detected. The initial mask is set to this rectangle to be sure that the whole skull is inside the mask. Then the algorithm is executed.

Assuming that the head is approximately symmetric, the symmetry axes is set to be parallel to the vertical axis and to divide the detected rectangle into two parts of the same size.

The results of the segmentation algorithm is not only the border of the skull, but also the border of the brain. This border is used to extract only the brain instead of the whole skull as in [2]. Only the segment that is located in the center is extracted. Because in some cases the brain segment can be joined to the skull segment but not symmetrically, another processing has to be done. The operation of logical conjunction is performed with this segment and its symmetric flipped image. This causes that points that are not on one side will not be considered also on the other side. The resulting mask is applied to the input image. The result of the brain extraction is shown in Figure 1.

The described process approximately extract the brain and set the symmetry axis in center of the new image. Except the brain, in cases where eyes are present, they are also inside the brain mask because

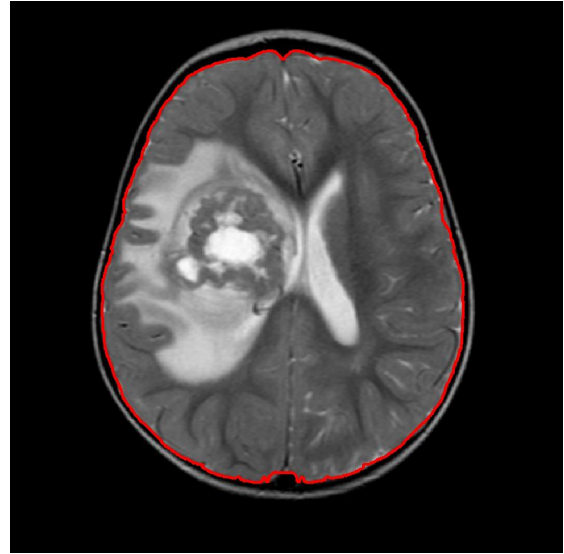


Figure 1. Extracted brain.

there is usually not clear border between them and brain.

Even if the mask is not so precise, the future results are not so influenced because the asymmetries caused by tumor are much higher.

After the extraction of the mask, the image is filtered by a Gaussian filter of size 5x5 to make the particular parts more homogeneous. The resulting mask is then applied to this filtered image followed by cutting the image because in parts outside the mask, the symmetry does not need to be checked.

2.2. Asymmetry detection

The main part of this work is the detection of symmetric anomalies, which are usually caused by brain tumor, whose detection is the main purpose of this article. The first step of this process is dividing of the input image into two approximately symmetric halves.

Assuming that the head is not rotated and the skull is approximately symmetric, the symmetry axis is parallel to vertical axis and divide the image of detected brain into two parts of the same size.

A squared block, with the side length computed as one quarter of the longer side of the input image, is created. This size is suitable for the detection of both small and large tumors. The algorithm goes through both halves symmetrically by this block. The step size is smaller than the block size to ensure the overlapping of particular areas. These areas are compared with its opposite symmetric part. In this case, the step size of one sixteenth of the block size was set.

Comparing is done by Bhattacharya coefficient. [1] Normalized histograms with the same range are computed from both parts and the Bhattacharya coefficient is computed from these histograms as follows [1]:

$$BC = \sum_{i=1}^N \sqrt{l(i) \cdot r(i)}, \quad (1)$$

where N denotes the number of bins in the histogram, l and r denote histograms of blocks in left and right half, respectively.

The range of values of Bhattacharya coefficient is $(0, 1)$, where the smaller value, the bigger difference between histograms. For the next computation, the asymmetry is computed as:

$$A = 1 - BC. \quad (2)$$

This asymmetry is computed for all blocks. The global maximum is detected. This is the most asymmetric block and most likely contains the tumor. Since the tumor can be larger, the initial size of the block, also the blocks with asymmetry bigger then $0.5 \cdot \max(Asym)$, are extracted. This threshold was set experimentally as a compromise between the size of the area and the asymmetry of areas. When the threshold was decreased, the resulting areas were too large, while for higher thresholds, some parts of the tumors were located outside the area.

The output of this computation is a both-sided mask containing the most asymmetric parts. This mask is slightly enlarged by morphological operation dilation for the case that some part of the tumor could be outside the region. This mask is applied to the input image.

The whole cycle is repeated twice for this new image but with smaller block. Height and width of the block is iteratively reduced to the half of the previous value. So the new size of the block is one quarter and one sixteenth of the initial size, respectively. The purpose of smaller areas is the more precise detection of asymmetry. This approach corresponds to multi resolution image analysis described in [11].

The resulting both-sided mask is again applied to the input image and this image is sent to the output of the detection process.

The results of particular steps are shown in the Figure 2. The input image size in this example was 256x256, so the Figures 2(a), 2(b) and 2(c) demonstrate detection of the most asymmetric areas for the

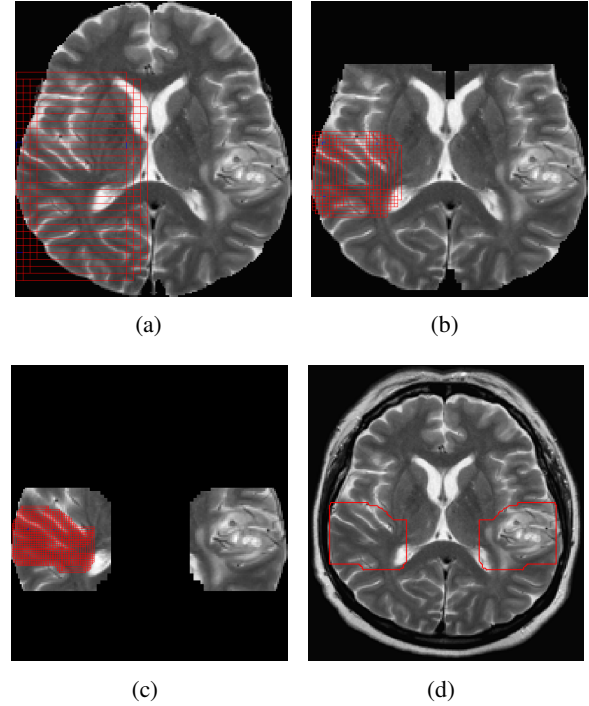


Figure 2. Asymmetries detection: (a) the first step for block size of 64x64 pixels, (b) the second step for block size of 32x32 pixels, (c) the third step for block size of 16x16 pixels, (d) the result of the asymmetries detection,

block size of 64x64, 32x32 and 16x16 pixels, respectively. As can be seen, searching for asymmetric parts is done only in asymmetric areas provided by previous step.

2.3. Locating the tumor

The detection of asymmetric areas does not explicitly locate the position of the tumor. There are still two possible locations of the tumor - right or left side. Two methods, for deciding in which part the tumor is, were tested. First of them is the prior-knowledge of the physical properties of brain tissues.

In T2-weighted images, tumors and edemas appear hyperintense [13]. This means that the produced signal is stronger than the signal of the white matter, in which tumors are located in most cases. This method is based on computation of the mean of the region. Tumors located near ventriculus could cause problems, because ventriculus produces even stronger signal. This could lead to misclassification.

The second possibility how to locate the tumor is to find it in the same way as asymmetries. Normalized histograms are computed from both areas and also from the rest of the brain. Histograms of both areas are compared with the rest of the brain using Bhattacharya coefficient. Area with less similar his-

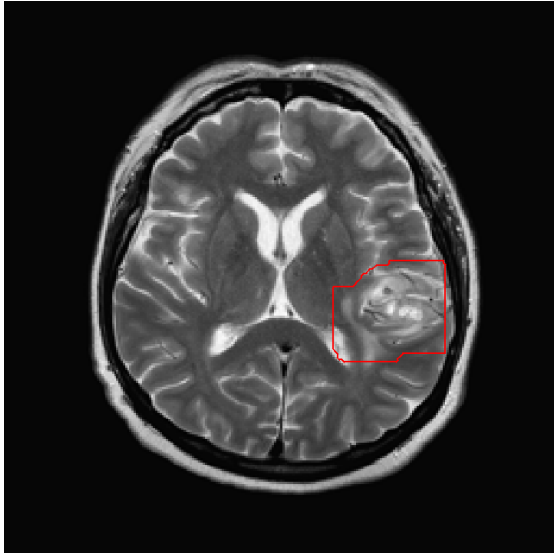


Figure 3. Located tumor.

togram is labeled as the one containing the tumor.

Both methods were tested. The first one produces slightly better results, the quantitative results are described in the next section.

The result of the tumor location for the input image from Figure 2(d) is shown in Figure 3. In this figure, the result image of the whole algorithm is demonstrated.

A problem occurs if the tumor appears in both halves of the brain. Since the tumor is not symmetric it is likely detected as asymmetric area even in this case. But the locating step relies on comparing both sides, therefore only one of them can be labeled as a pathological.

3. Results

The algorithm was tested on 73 T2-weighted images from 13 different patients. Every image contained a tumor, a tumor with an edema or only the edema. Various shapes, locations, and sizes of these pathological areas and various image resolution were tested. Results are shown in Table 1. Results are described by number of cases and by percentage of the total number of tested images.

At first, the evaluation of the detection of symmetric anomalies will be described. In 1 case, the anomaly detection failed. In this particular image, only the edema was present and it was hardly visible even for human. At least 75% of the pathological area was detected in 72 cases. In 8 cases, the pathological area was found, but the extracted area was too large compared to the tumor, or the tumor

Result	Num. of cases	Percentage
Number of images	73	
Incorrect anomaly detection	1	1.37%
Detected main part of path. area	72	98.63%
Too large area	8	10.96%
15-20% outside	9	12.33%
Correct anomaly detection	55	75.34%
Correct area extraction	52	71.23%

Table 1. Total results.

was not in the approximate center of this area. The example of this result is shown in Figure 7(b). In 9 cases, the pathological area was found, but from 15% to 25% of it was situated outside the extracted area. This includes also 3 images, where the pathological area was located in both halves. Such case is shown in Figure 7(a). In only 2 of these 9 cases, more than 20% of the pathological area was located outside the extracted region. It means that in 17 cases, the result of anomaly detection was not totally incorrect, but it was not so accurate. In 55 cases, the anomaly detection was correct.

After the anomaly detection process, the decision, on which side the pathological area is, has to be done. In this part, only 55 images with correct anomaly detection result are considered. The region mean computation failed in 3 cases, so the total number of correctly extracted area is 52. For localizing the tumor by comparing to the rest of the brain, computation failed in 6 cases, so the total number of correctly extracted area is 49.

In Table 2, the results dependent on pathological area size are shown. There were 8 small, 23 medium and 42 large tumors. According to the assumption, the most of tumors, whose part was situated outside the extracted region, belongs to the group of large pathological area, and the only totally incorrect result belongs to the group of small pathological area.

A few results can be seen in the Figure 4, 5 and 6. The area of the tumor location is surrounded by a red line. One can see that the detected area is a little bit larger than the pathological area itself. One reason is the use of dilation at the end of asymmetry detection. This is done to locate the whole tumor and not only a part of it. Another reason could be explained by

Result	Size of pathological area		
	Small	Medium	Large
Number of images	8	23	42
Incorrect anomaly detection	1	0	0
Detected main part of path. area	7	23	42
Too large area	2	4	2
15-20% outside	0	1	8
Correct anomaly detection	5	18	32
Correct area extraction	5	17	30

Table 2. Results dependent on tumor size.

influence of the tumor in the neighbor parts of the brain. Because the tumor is a tissue which is growing during the time, it presses the other parts of the brain. This creates the deformation and asymmetry not only in the tumor location but also in the adjacent parts and gradually in the whole brain.

Since the method is based on asymmetry detection, the problem appears when the tumor is located in both halves or on the symmetry axis. In this case, some parts of the tumor could be outside of the extracted area even if they are located in the half in which the tumor was detected. The reason is that the tumor located in both sides causes symmetry in these parts, so for the algorithm it seems to be a healthy tissue.

The part of the tumor located in the other half of the brain is also outside the detected area. The example of that problematic type of tumors is shown in the Figure 7(a). This problem could be prevented by an additional step that consists of checking whether the border of the asymmetric area matching the symmetry axis border, in other words if the both-sided mask creates only one homogeneous region.

Compared to the approach proposed in [2], our algorithm provides a region containing the most of the tumor area, which will be necessary in the next processing that is the aim of the future work. Moreover, the results of our method are not simple rectangles, but they can better capture the structure of the tumor.

From the principle, the proposed algorithm could also detect multifocal tumors as separated regions [14]. Unfortunately, this assumption was not tested, because no images containing multifocal tumors were present.

4. Conclusion and future work

The aim of this work was not the precise segmentation of the brain tumor but only detection of approximate location of the tumor. This location could be then used for more precise tumor extraction and could make this task easier.

The future work will consist of the automatic symmetry axis detection and the more precise extraction of the tumor based on current results.

The attention in the future work will also be paid on automatic detection of the image containing the brain tumor and searching for the relations between neighbor slices. After that, the work will continue with extending the method to 3D MR images.

5. Acknowledgments

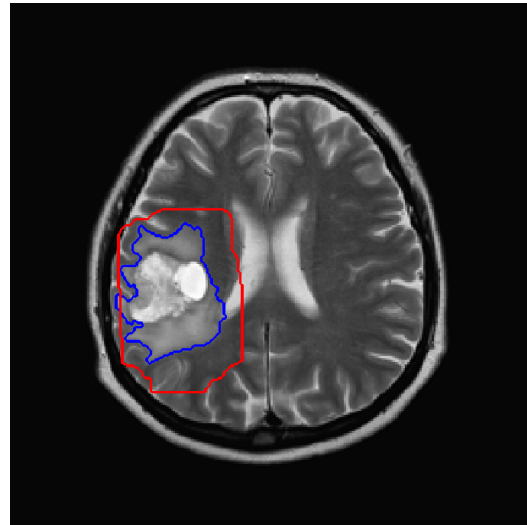
This research is part of the project reg. no CZ.1.07/2.3.00/20.0094 "Support for incorporating R&D teams in international cooperation in the area of image and audio signal processing" and is co-financed by the European Social Fund and the state budget of the Czech Republic.

References

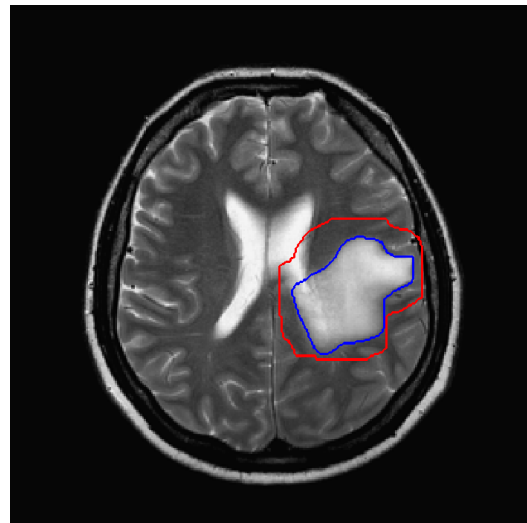
- [1] Bhattacharyya, A., "On a measure of divergence between two statistical populations defined by their probability distribution," *Bulletin of the Calcutta Mathematical Society*, vol. 35, pp. 99–110, 1943. 3
- [2] Ray, N. and Saha, B.N. and Graham Brown, M.R., "Locating Brain Tumors from MR Imagery Using Symmetry," *Signals, Systems and Computers, 2007. ACSSC 2007. Conference Record of the Forty-First Asilomar Conference on*, pp. 224–228, November 2007. 2, 5
- [3] Khotanlou, H. Colliot, O. and Bloch, I., "Automatic brain tumor segmentation using symmetry analysis and deformable models," *Conf. on Advances in Pattern Recognition ICAPR, Kolkata, India*,. Jan. 2007. 1
- [4] Pedoia, V., Binaghi, E., Balbi, S., De Benedictis, A., Monti, E., et al., "Glial brain tumor detection by using symmetry analysis," *CProc. SPIE 8314, Medical Imaging 2012: Image Processing, 831445*,. February 23, 2012. 1
- [5] Somasundaram, K., Kalaiselvi, T., "Automatic detection of brain tumor from MRI scans using maxima transform," *National Conference on Image Processing (NCIMP) 2010*. 1
- [6] Zhang, J. G., Ma, K. K., Er, M. H., and Chong, V., "Tumor segmentation from magnetic resonance imaging by learning via one-class support vector

machine,”*International Workshop on Advanced Image Technology (IWAIT 2004)*., pp. 207–211, 2004. 1

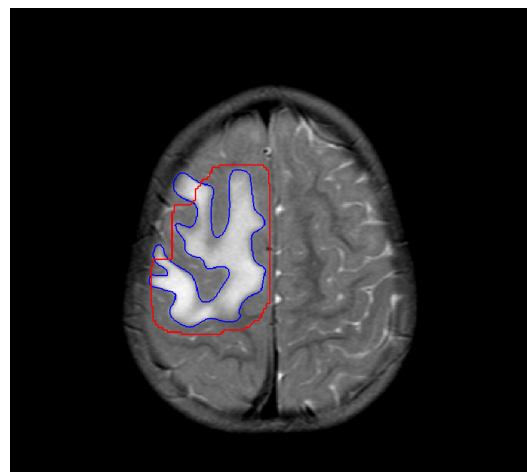
- [7] Cuadra, M. B., Pollo, C., Bardera, A., Cuisenaire, O., Villemure, J. G. and Thiran, J. P., *Atlas-based segmentation of pathological MR brain images using a model of lesion growth.*, *IEEE Trans. Med. Imaging.*, vol. 23, num. 1, pp. 1301–1314, 2004 1
- [8] Ruppert, G. C. S., Teverovskiy, L., Yu, C., Falcao, A. X., Liu, Y., “A New Symmetry-based Method for Mid-sagittal Plane Extraction in Neuroimages” *International Symposium on Biomedical Imaging: From Macro to Nano*, 2011. 2
- [9] Xu, C. and Prince, J. L., “Snakes, shapes, and gradient vector flow.” *IEEE Transactions on Image Processing*, vol. 7, num. 3, pp. 359–369, 1998. 2
- [10] Capelle, A. S., Colot, O., and Fernandez-Maloigne, C., “Evidential segmentation scheme of multi-echo MR images for the detection of brain tumors using neighborhood information.” *Information Fusion*.vol. 5, pp. 103–216, 2004. 1
- [11] Kropatsch, W. G., Haxhimusa, Y., Ion, A., “Multiresolution Image Segmentations in Graph Pyramids,” in *Applied Graph Theory in Computer Vision and Pattern Recognition Studies in Computational Intelligence*, vol. 52, pp. 3–41, 2007. 3
- [12] Rodriguez, A. O., “Principles of magnetic resonance imaging.”*Revista Mexicana de Fisica*, 2004.
- [13] Shah, L. M., Salzman, K. L., “Imaging of Spinal Metastatic Disease.”*International Journal of Surgical Oncology*, 2011. 3
- [14] Lim, D. A., Cha, S., Mayo, M. C., Chen, M.-H., Koles, E., VandenBerg, S., Berger, M. S., “Relationship of glioblastoma multiforme to neural stem cell regions predicts invasive and multifocal tumor phenotype,” in *Neuro Oncol*, vol. 9, Issue. 4, pp.424–429, October 2007. 5



(a)

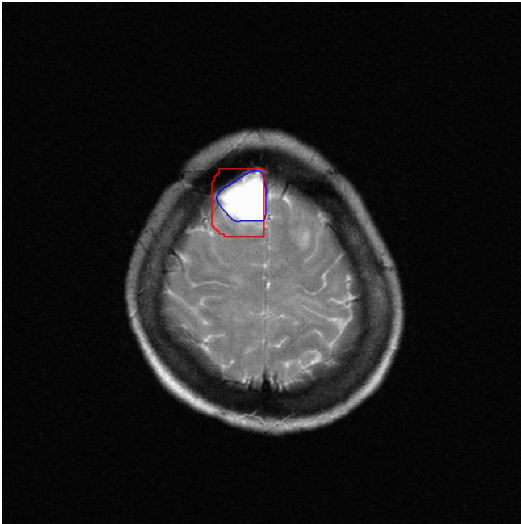


(b)

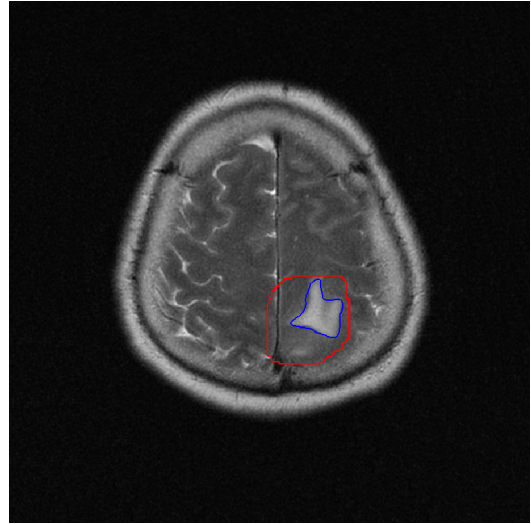


(c)

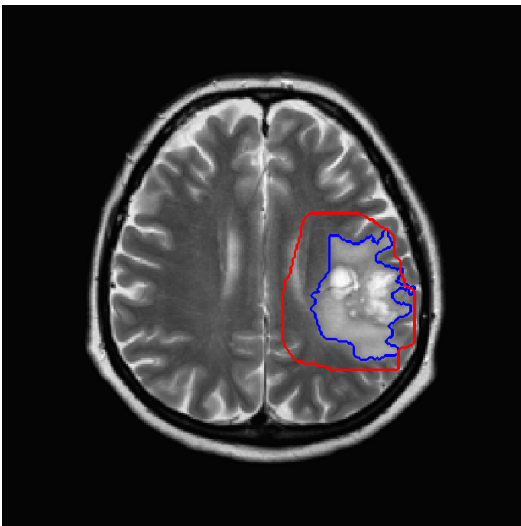
Figure 4. Examples of results (red area) compared to the ground truth (blue area).



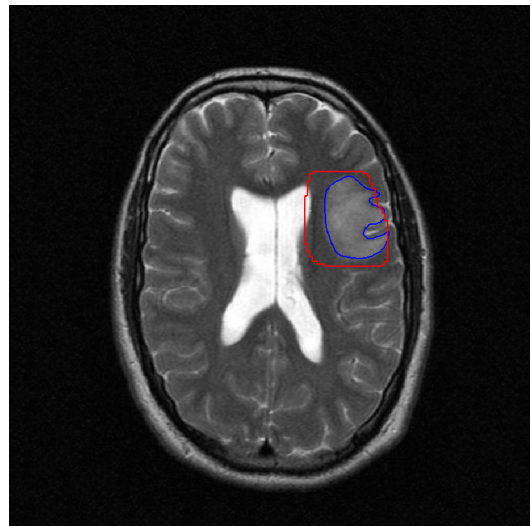
(a)



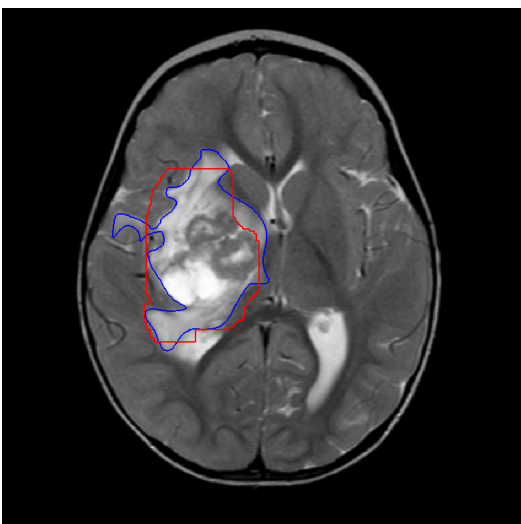
(a)



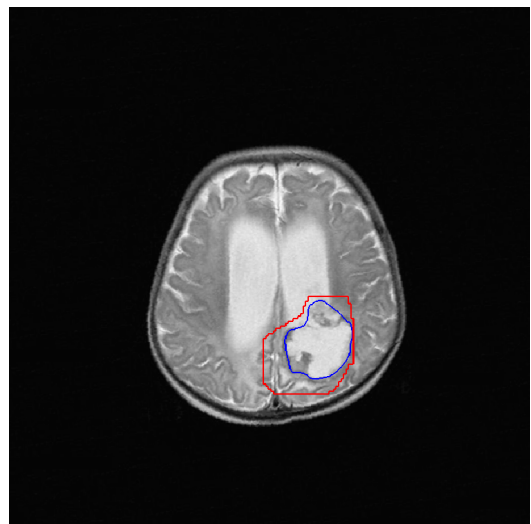
(b)



(b)



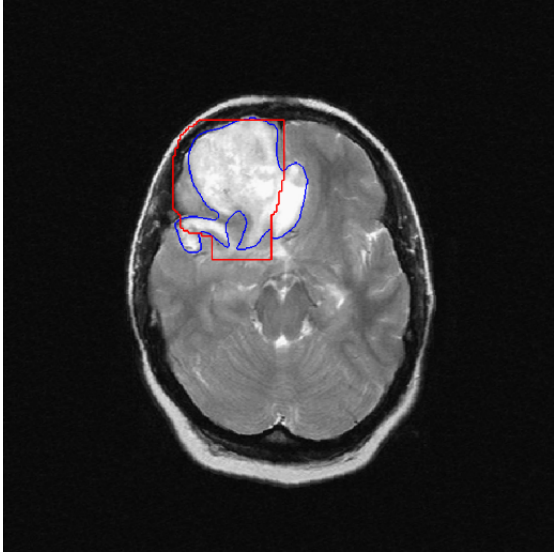
(c)



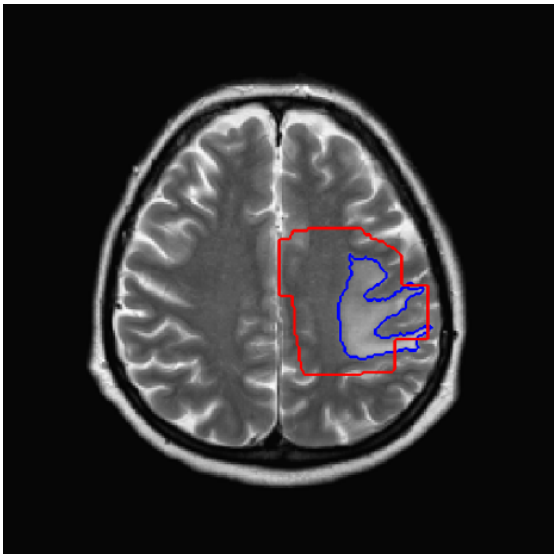
(c)

Figure 5. Examples of results (red area) compared to the ground truth (blue area).

Figure 6. Examples of results (red area) compared to the ground truth (blue area).



(a)



(b)

Figure 7. Less precise results (red area) compared to the ground truth (blue area): (a) Problematic type of tumor located in both halves, (b) Result evaluated as a large area.